Bergado, D. T., Shivashankar, R., Alfaro, M. C., Chai, J.-C. & Balasubramaniam, A. S. (1993). *Géotechnique* **43**, No. 4, 589–603

Interaction behaviour of steel grid reinforcements in a clayey sand

D. T. BERGADO,* R. SHIVASHANKAR,† M. C. ALFARO,* JIN-CHUN CHAI* and A. S. BALASUBRAMANIAM*

The interaction behaviour between steel grid reinforcements and a clayey sand has been studied in laboratory and field pullout tests. The clayey sand is potentially useful as cheap, low quality, locally available and cohesive-frictional backfill in the construction of mechanically stabilized earth walls and embankments, especially in coastal areas. The laboratory tests were conducted under undrained conditions at three compaction moisture conditions. The field tests were conducted on dummy reinforcements embedded at different elevations in a full-scale test embankment resting on soft clay foundation. The laboratory tests revealed that the moisture content of the compacted soil, compaction stress, applied normal stress level, diameter and spacing to diameter ratios of the transverse members of the steel grid, all affect the soil–reinforcement interaction, and thereby, also the magnitudes of the pullout resistances. Interferences between the bearing transverse members of the grid were found to be less significant for spacing to diameter ratios above 75. The laboratory tests, in general, gave conservative values of the pullout resistances as compared with the field tests. The proposed prediction equations agreed well with the experimental data.

KEYWORDS: bearing capacity; compaction; earthfill; full-scale tests; laboratory tests; reinforced soils.

L'interaction entre les renforcements par treillis métalliques et les sables argileux a été étudiée à l'aide d'essais de traction en laboratoire et sur chantier. Le sable argileux est utilisé pour construire des murs en terre mécaniquement stabilisés et des remblais, dans les zones littorales notamment. Ce type de matériau est en effet un matériau de remplissage cohérent-frottant bon marché, de qualité médiocre et disponible localement. Les essais de laboratoire ont été menés, dans des conditions non-drainées, avec trois teneursen eau de compactage. Les essais de chantier ont été réalisés sur des renforcements ancrés à différentes profondeurs dans un remblai grandeur nature reposant sur des argiles molles. Les essais de laboratoire ont montré que la teneur en eau du sol compacté, la contrainte de compaction, le niveau de contrainte normale, le diamètre et les rapports espacement-diamètre des composants transversaux du treillis métallique jouent sur les interactions renforcement-sol, et par conséquent, sur la grandeur de la résistance à la traction. Les interférences entre les éléments porteurs transversaux du treillis semblent moins importantes pour des rapports espacement–diamètre supérieurs à 75. Les essais de laboratoire donnent, en général, des valeurs de résistance en traction plus reproductibles que celles obtenues dans les essais de chantier. Les équations proposées pour la prédiction du comportement sont en bon accord avec les données expérimentales.

INTRODUCTION

The use of cheaper and locally available soils as backfills in mechanically stabilized earth (MSE) constructions, although these may be of low quality, is necessary in regions where good quality granular backfill soils are not readily available at a reasonable cost. MSE is a composite construction material formed by the inclusion of tension resistant materials in the backfill soils to impart tensile strength to the soil and to improve its engineering properties. In its modern form, MSE was first applied for retaining walls that utilized granular backfills and horizontally laid steel strip reinforcements connected to concrete facing units, and was called 'reinforced earth' (Vidal, 1969). Since then, soil reinforcement techniques have developed greatly through the use of various forms of reinforcement of different materials and in different applications. The use of low quality, locally available and cohesive–frictional backfills in MSE constructions has attracted much attention in recent years with the advent of the grid type of reinforcement, and

Discussin on this Paper closes 5 April 1994; for further details see p. ii.

* Asian Institute of Technology, Bangkok.
† Saga University, Japan.

especially the welded wire reinforcements. Chang, Hannon & Forsyth (1977) observed that the steel grid reinforcements generated about 5–6 times more pullout resistance than steel strip reinforcements of equivalent area, and that about 85–90% of the total pullout resistance F_t of the steel grid reinforcements comes from the passive resistance F_b due to the soil bearing in front of the transverse members of the grid.

The transverse members of a grid reinforcement can be considered analogous to a series of strip footings in succession which have been rotated through 90° to the horizontal and pulled through the soil. Two types of bearing capacity failure mechanism in front of the transverse members of the grid reinforcement have been proposed. The first is the general bearing capacity failure mechanism (Peterson & Anderson, 1980) in which the slip planes are fully developed (Fig. 1). The prediction equation for the pullout resistance in this case is based on the Terzaghi–Buisman bearing capacity equation as follows

$$F_b/NWD = CN_c + \sigma_v N_q \quad (1)$$

where N, W and D are the number, width and diameter respectively of the transverse wires of the grid reinforcement, C is the cohesion intercept of the backfill soil, σ_v is the vertical normal stress and

$$N_q = e^{\pi \tan \phi} \tan^2 (45 + \phi/2) \quad (2)$$

$$N_c = (N_q - 1) \cot \phi \quad (3)$$

where ϕ is the angle of internal friction of the backfill soil. This prediction gives an apparent upper bound envelope for the pullout capacities of the grid reinforcements (Palmeira & Milligan, 1989; Jewell, 1990; Shivashankar, 1991). The second mechanism, proposed by Jewell, Milligan, Sarsby & Dubois (1984) is based on the punching shear failure mode of deeply embedded foundations (Fig. 2). The equation for calculating the pullout bearing resistance has the same form as equation (1), but the bearing capacity factors are expressed as N_{q1} and N_{c1} where

$$N_{q1} = e^{(\pi/2 + \phi) \tan \phi} \tan (45 + \phi/2) \quad (4)$$

$$N_{c1} = (N_{q1} - 1) \cot \phi \quad (5)$$

This prediction gives an apparent lower bound envelope for the pullout capacities of the grid reinforcements (Palmeira & Milligan, 1989; Jewell, 1990; Shivashankar, 1991).

Ospina (1988) observed that in the case of dry sands, at low confining pressures the failure was close to the punching shear failure mode, whereas at higher confining normal pressures the failure approached a general bearing failure. Using radiography, Ospina observed a general bearing failure with backfill soils comprising uniformly graded fine sand (sand A) and well graded coarse-to-fine sand (sand B) in their loose states. In the dense state, sand A predominantly showed a punching failure; sand B showed a combination of punching and general bearing failures. For the dry Leighton Buzzard sands used in their pullout tests, Palmeira & Milligan (1989) observed that the interference becomes negligible for S/D values above 50, where S is the spacing between the grid bearing members. The data and analyses presented in this Paper were obtained by Shivashankar (1991).

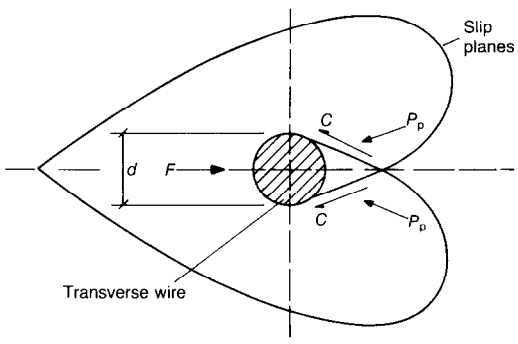

Fig. 1. General bearing capacity failure mechanism (Peterson & Anderson, 1980): see equation (2)

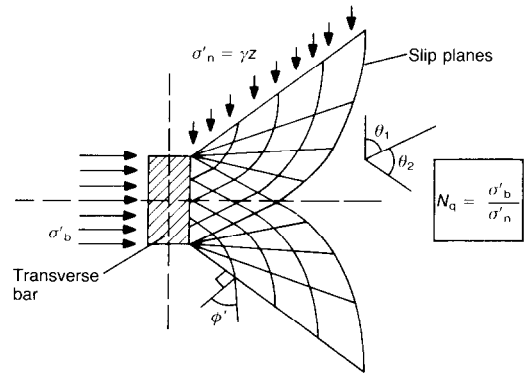

Fig. 2. Punching shear failure mechanism (Jewell *et al.*, 1984): see equation (4)

CLAYEY SAND BACKFILL

The index properties of the clayey sand backfill are given in Table 1. The results of the direct and the triaxial shear tests are summarized in Table 2. Direct shear tests were conducted at three moisture conditions: at the dry and wet sides of optimum moisture content (OMC) compacted so

Table 1. Index properties of clayey sand

Colour	Brownish
Percentage passing US standard sieve 200	45%
Atterberg limits	
Liquid limit	32%
Plastic limit	12%
Standard Proctor compaction test	
OMC	14·4%
Maximum dry density	17·9 kN/m^3
Specific gravity of soil particles	2·55

that the dry density corresponded to 95% of standard Proctor density, and at OMC compacted to 100% of standard Proctor density (Table 2). The direct shear specimen is 150 mm long, 150 mm wide and 127 mm high. The air dried soil sample was mixed with the appropriate amount of water, then sealed in a plastic bag and kept in a humid room for 24 h. The specimen was compacted to the desired degree in the direct shear box in four layers. Normal pressure was applied and the specimen was sheared at a constant shear displacement rate of 1 mm/min. The tests were conducted in unconsolidated–undrained conditions to simulate the shear condition of the soil during the pullout test. However, the triaxial tests were conducted only at a moisture content of 13·2%, about 1% on the dry side of optimum, and compacted to 95% of standard Proctor density. The specimen was 102 mm in diameter and 204 mm high, and was compacted in a mould by a static compaction machine. The tests were conducted in unconsolidated–undrained conditions with a constant axial strain rate of 0·019%/min (0·38 mm/min). The strength parameters in Table 2 were determined by total stress analysis. Typical stress–strain curves from the direct and the triaxial shear tests are shown in Figs 3(a) and 4. Fig. 3(b) shows the failure envelopes from the direct shear tests at all three moisture conditions. The typical grain size distribution of the clayey sand used in this study is shown in Fig. 5.

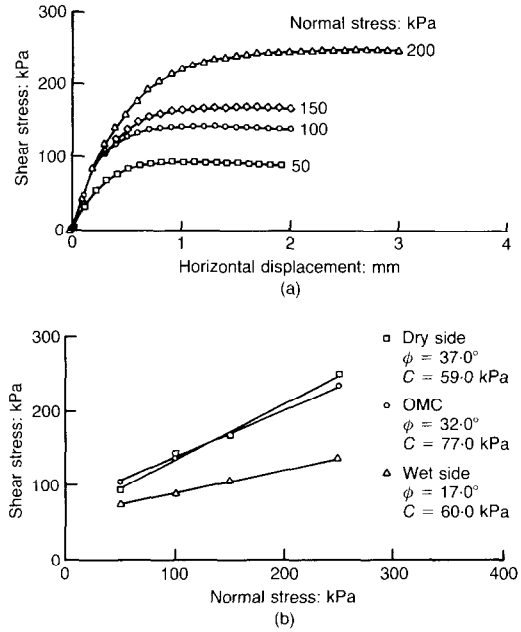

Fig. 3. (a) Typical stress–strain curves from the direct shear tests (clayey sand (95%) on dry side); (b) failure envelopes from the direct shear tests at various compaction moisture conditions

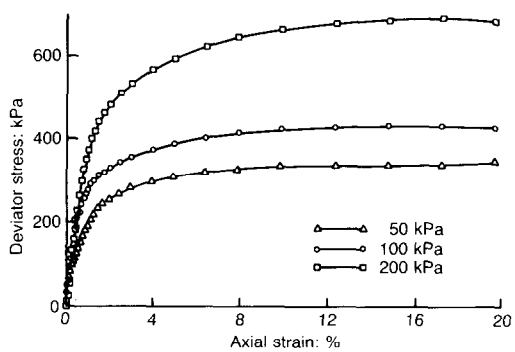

Fig. 4. Typical stress–strain curves from triaxial shear tests: clayey sand (95%) on dry side

Table 2. Direct and triaxial shear results for clayey sand

Standard Proctor density	Water content: %	Dry unit weight: kN/m^3	ϕ: degrees	C: kPa
Direct shear test				
95% dry side	10·0	17·0	37·0	59·0
100% (OMC)	14·4	17·9	32·0	77·0
95% wet side	20·2	17·0	17·0	60·0
Triaxial test				
95% dry side	13·2	17·0	33·0	56·0

Clay	Silt	Sand			Gravel	
		Fine	Medium	Coarse	Fine	Coarse
33	11	41	14	1	0	0

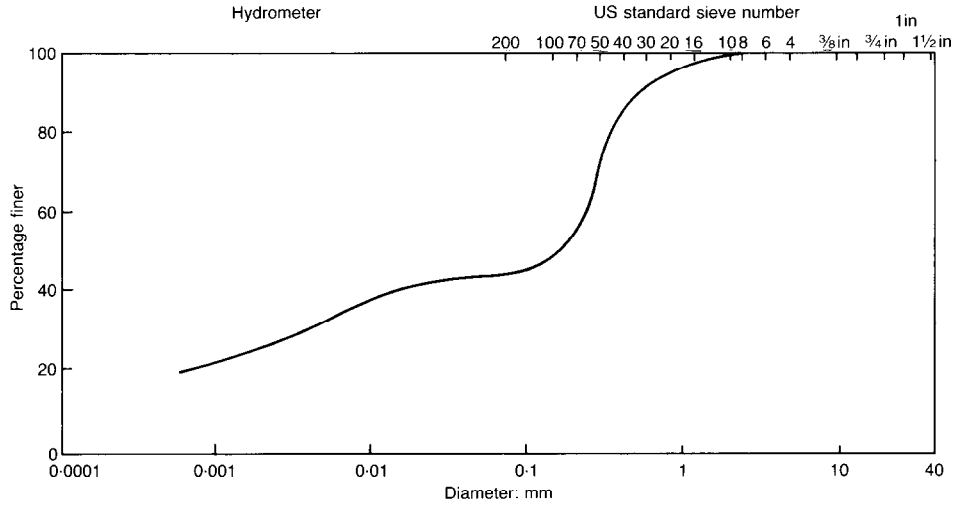

Fig. 5. Grain size distribution of clayey sand (1 in = 25·4 mm)

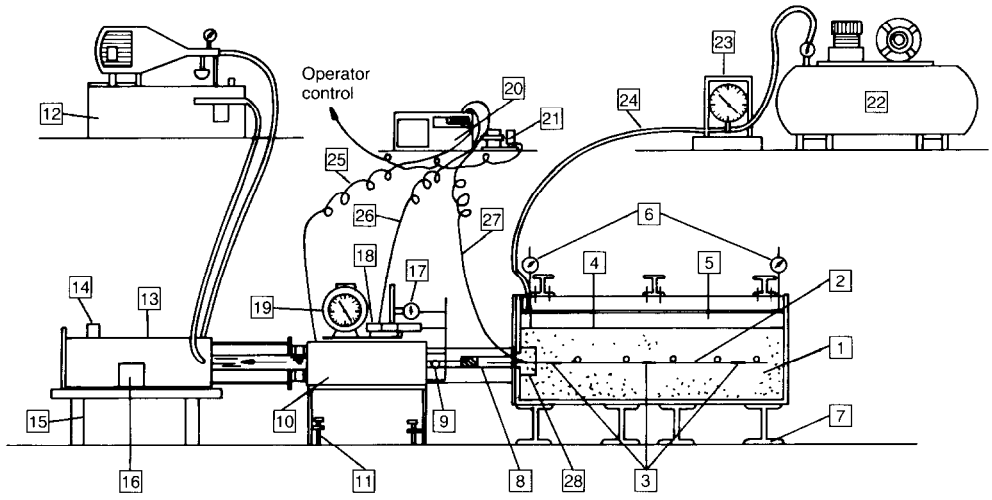

1 Compacted soil in pullout box
2 Grid specimen
3 Strain gauges
4 Flexible plate placed over compacted soil
5 Air bags for applying normal pressures
6 Dial gauges at top to measure dilatancy
7 Airlock pads
8 Clamping mechanism
9 Swivel joint
10 Load cell
11 Mount load for load cell of adjustable height
12 Piston pump and motor with filters and valves
13 Hydraulic cylinder
14 Servo valve
15 Mount for cylinder
16 Analogue output module
17 Front dial gauges
18 LVDT for measuring front displacements
19 Stop clock
20 21X data logger with multiplexer
21 EMRS power supply module and EMD amplifier module
22 Air compressor
23 Regulator
24 Stiff tubing
25 Lead wire connecting load cell to data logger
26 Lead wire connecting LVDT to data logger
27 Lead wires connecting all strain gauges to data logger through multiplexer
28 Two horizontal sleeves 100 mm apart

Fig. 6. Laboratory pullout test set-up

LABORATORY TESTS

Pullout tests were conducted in the laboratory using a pullout box 1·25 m long, 0·75 m wide and 0·51 m deep (inside dimensions), made of steel plates and steel beams welded and bolted together (Fig. 6). A multi-stage pullout testing procedure was followed. Three pullout tests in three corresponding loading stages were conducted at each set-up. The vertical confining normal stress was increased at each stage. In the first stage, the reinforcing mat was pulled out under a given normal stress, then the pulling force was released and the normal stress was increased. After allowing the normal stress to stabilize for ~30 min, the mat was again pulled out. This constituted the second stage, and was followed by a similar third stage. At each stage the mat was pulled out by 25 mm.

Two diametrically opposed strain gauges were fixed at each instrumentation point on the grid specimen to cancel any bending stresses. Before the start of the actual pullout test, a seating load of ~2 kN was applied to remove any slack in the system. During the pullout test, a uniform pullout rate of 1 mm/min was maintained with the help of electronic controls. All the pullout tests were conducted under unconsolidated–undrained conditions. The clayey sand on the dry side of optimum and at the OMC was actually in the partially saturated state. Two types of pullout test (or reinforcement) were conducted.

(*a*) *friction pullout tests:* conducted using a reinforcement system with the four longitudinal bars spaced laterally at 0·15 m and no transverse bars embedded in the soil (Fig. 7(a))

(*b*) *grid pullout tests:* conducted using welded wire grid reinforcements of varying bar sizes and mesh geometries (Fig. 7(b), Table 3); the contribution of the bearing resistances in front of the transverse members was estimated by subtracting from the results of the grid pullout test (total pullout resistance) the frictional pullout resistance derived from the corresponding friction pullout test in (*a*) above.

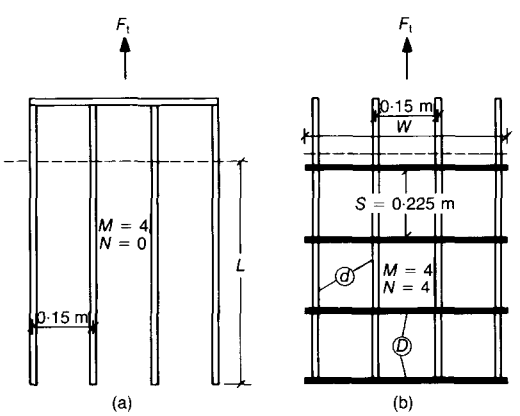

Fig. 7. Types of reinforcement used in the laboratory pullout tests

Table 3. Diameter of welded wires

Wire size number	Nominal diameter: mm
W3·5	5·359
W4·5	6·071
W5	6·502
W7	7·595
W12	9·931

In each set-up, the soil in the pullout box was compacted in two equal lifts, each 0·15 m thick, using a hand-operated impact (Wacker) tamper. After compaction of the first lift, the level of the compacted soil surface reached almost up to the centre of the pullout slot where the reinforcement was placed. The grid specimen was then placed in position at the centre of the slot and its level and alignment were checked. The second lift of the backfill soil was placed over it and compacted again. The uniformity in the degree of compaction and the moisture contents in both lifts was checked by use of a nuclear gauge densitometer.

Pullout tests were conducted at the same three compaction moisture conditions as for the direct shear test specimens. A variation of ±2% about the mean value was observed in the degree of compaction; a corresponding variation of ±1% was recorded in the moisture content (Fig. 8). The clayey sand used was found to be very sensitive to changes in moisture content only on the wet side of optimum, where there was a sharp decrease in shear strength (Fig. 3(b)).

Two horizontal metal plates were used as sleeves on the inside part of the opening of the pullout box, extending 0·15 m behind the face. The purpose of these was to decrease the horizontal stresses on the front face near the slot during the pullout and also to minimize the arching effects over the grid specimens. The sleeves were positioned across the full width of the pullout box, above and below the reinforcements. This also kept the normal loads off the front 0·15 m. The two sleeves were separated by spacers 0·1 m high at the front corners of the pullout box to avoid any contact with the reinforcements as shown in Fig. 6.

A layer of fine sand ~30 mm thick was laid out on top of the compacted soil to distribute the normal pressure uniformly. The lower top cover plate, 6·35 mm thick, was then placed over the

sand. An inflated air bag was placed over this plate to take reaction from I-beams above it which were bolted onto the top of the pullout box, through an upper top cover plate.

FULL-SCALE TEST EMBANKMENT

A full-scale wall/embankment MSE system with welded steel geogrid reinforcements as shown in Fig. 9 was constructed inside the campus of the Asian Institute of Technology 42 km north of Bangkok. It has a vertical welded steel grid facing the front and a sloping back (Fig. 8(b)): the unreinforced slope can be built as 1 : 1 because of the effect of cohesion of backfill soil. It comprises three sections corresponding to the three different backfill materials used, i.e. clayey sand in section I, lateritic residual soil in section II and weathered Bangkok clay in section III (Fig. 9(a)). The backfill materials were compacted to 95% standard Proctor (ASTM D698) densities on the dry side of optimum (see Fig. 9). Details of the performance of this MSE wall/embankment have been given by Bergado, Sampaco, Shivashankar, Alfaro, Anderson & Balasubramaniam (1991), and Bergado, Shivashankar, Sampaco, Alfaro & Anderson (1991).

Related laboratory and field pullout test results using steel grid reinforcements in conjunction with this full-scale test embankment have been given by Bergado, Hardiyatimo, Cisneros, Chai, Alfaro, Balasubramaniam & Anderson (1992) and Bergado, Lo, Chai, Shivashankar, Alfaro & Balasubramaniam (1992). Dummy reinforcement specimens protruding ~0·35 m from the vertical face of the wall/embankment system were installed during construction, at different levels in each of the three sections, for field pullout tests. The foundation subsoil consists of a layer of soft clay ~6 m thick sandwiched between a surficial 2 m thick layer of weathered Bangkok clay and an underlying layer of stiff clay.

FIELD TESTS AND RESULTS

Constant strain field pullout tests were conducted about eight months after the construction of the test embankment. By this time, both the foundation subsoil and the wall/embankment system had undergone vertical and lateral movements. Five dummy reinforcement specimens embedded in the clayey sand section (see Fig. 9(a)) were pulled out. A typical dummy reinforcement is shown in Fig. 10. The pullout test procedure was the same as adopted in the laboratory pullout tests; the dummy reinforcements were pulled out at 1 mm/min. The pullout force was applied by means of a specially designed reaction frame butting against the wall face. A wooden platform was built to support the pullout equipment.

Figure 11 shows a typical set-up for the field pullout test. Figs 12 and 13 show the load–displacement and strain–displacement curves for the field pullout tests in clayey sand. These figures show that for dummy mats 7 and 9, the pullout resistance was not fully mobilized even at a pullout displacement of 125 mm. However, the increase in pullout resistance rate was reduced starting at a pullout displacement of 80 mm. Dummy mat 10 has longitudinal bars with ribs only (25 mm long) with 225 mm spacing. The

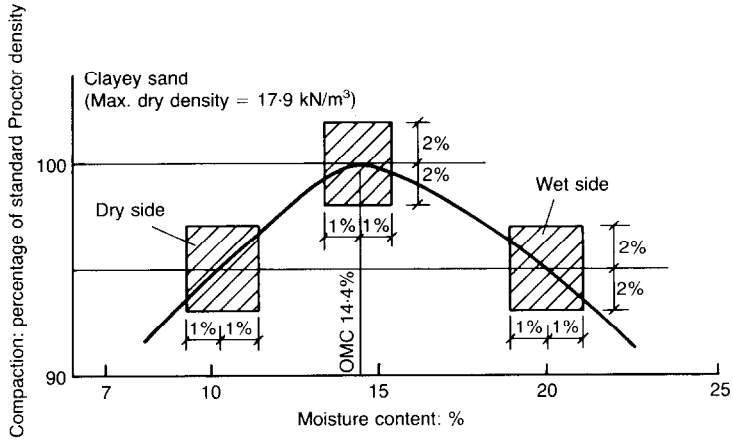

Fig. 8. Compaction curve of the clayey sand showing ranges of the moisture contents and the dry densities used in the laboratory pullout tests and the direct shear tests

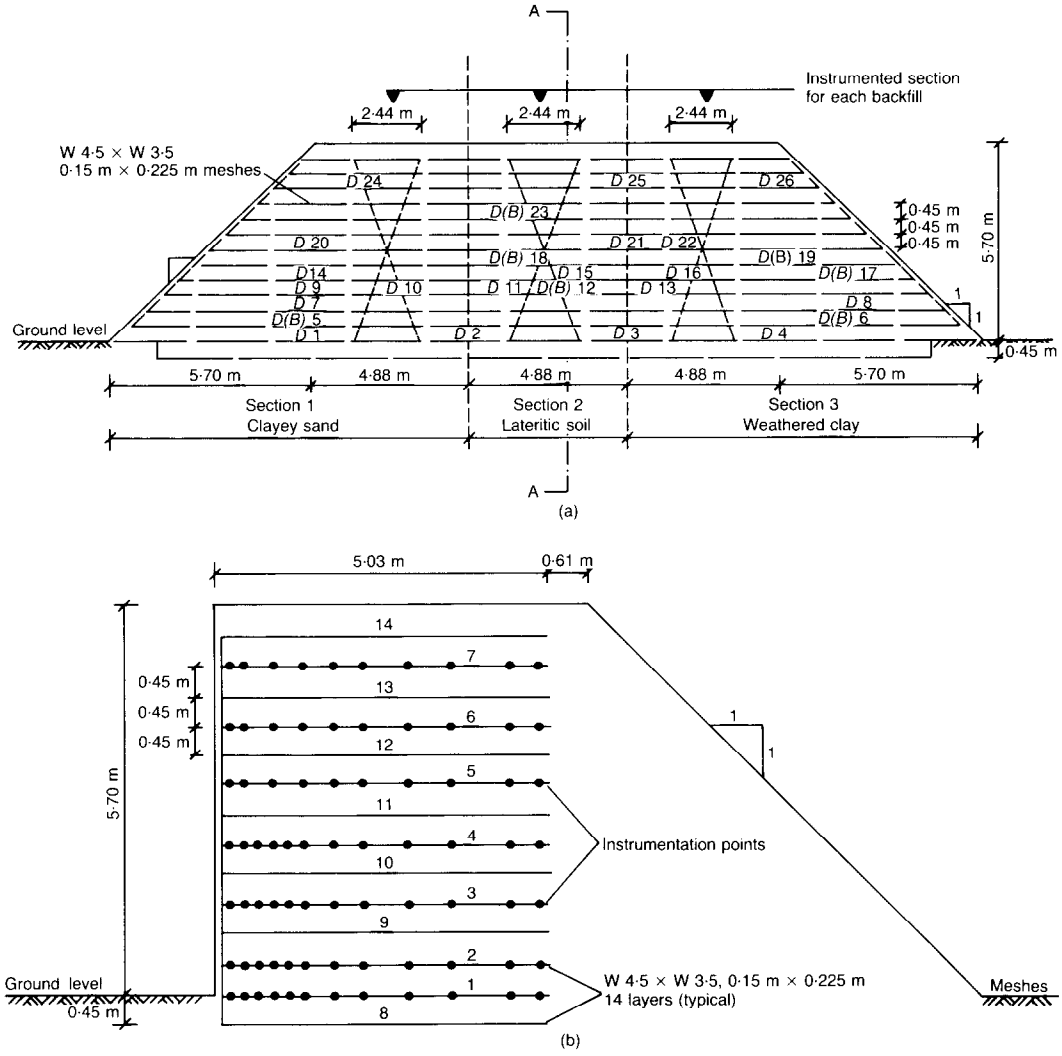

Fig. 9. Views of the welded wire wall: (a) front-sectional; (b) cross-sectional (only mats 1–7 are instrumented)

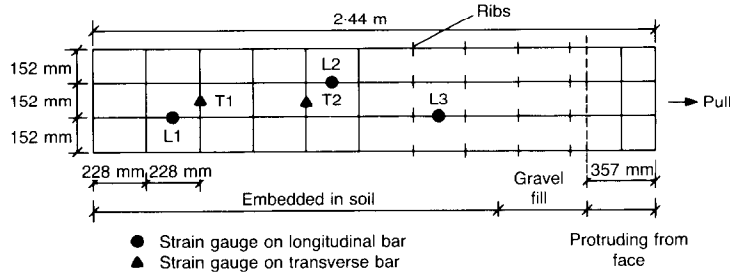

Fig. 10. Typical dummy reinforcement used in field pullout test

Fig. 11. Typical field pullout test set-up

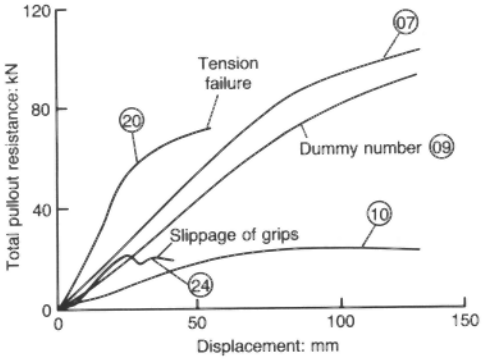

Fig. 12. Load–displacement curves from field pullout tests in clayey sand

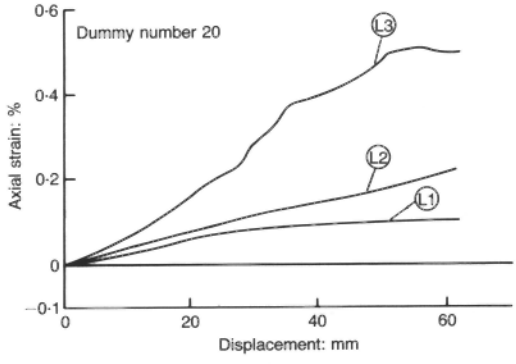

Fig. 13. Strain–displacement curves from field pullout tests in clayey sand

total resistance was fully mobilized at a pullout displacement of 60 mm. A comparison of the results from dummy mats 9 and 10 shows that most pullout resistance was derived from bearing resistance of grid transverse members. To be mobilized, the pullout bearing resistance needs larger pullout displacements.

LABORATORY TEST RESULTS

Friction pullout tests

Figure 14 shows the results of the friction pullout tests at various compaction moisture conditions. The frictional resistances $F_f/\pi LMd$ were found to increase slightly with increasing applied normal stress at all moisture conditions.

Apparent friction coefficient

The apparent friction coefficient on the longitudinal wires has been defined as

$$\mu^* = f/\sigma_{ave} \tag{6}$$

$$f = F_f/M\pi dL \tag{7}$$

where μ^* is the apparent friction coefficient, f is the frictional resistance over the longitudinal wires, σ_{ave} is the average overburden pressure on the members of the grid reinforcement, F_f is the maximum pullout force from the frictional pullout tests at the end of a 25 mm pull, M and D are the number and diameter of longitudinal wires in the grid reinforcement and L is the length of embedment of the grid reinforcement in the backfill soil. μ^* was found to decrease with the increase in the applied normal stress level. Fig. 15

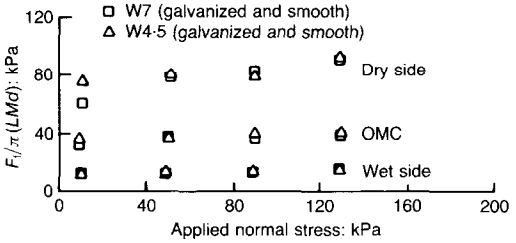

Fig. 14. Friction pullout test results for clayey sand at various moisture conditions (laboratory)

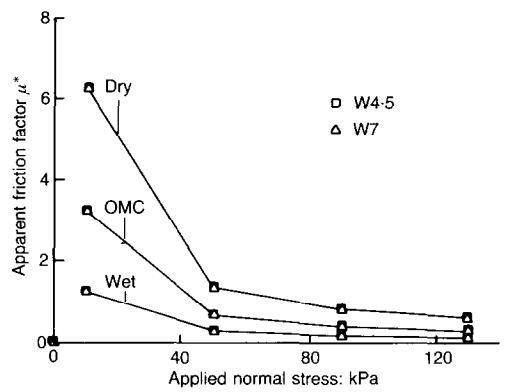

Fig. 15. Variation of the apparent friction coefficient with the applied normal stress level at various moisture conditions (laboratory, clayey sand)

shows that the curves flatten out beyond a normal stress level of ~100 kPa. These results are similar to those obtained by Schlosser & Elias (1978) for pullout tests of strip reinforcements from reinforced earth walls.

The average overburden pressure σ_{ave}, i.e. stress normal to the surface of the wires, was taken as 1·15 times σ_v (see Fig. 16) to account for the compaction induced stresses and the circular cross-section of the longitudinal wires. Compaction effects can be a form of overconsolidation. An assumed overconsolidation ratio of 8 was found to be appropriate for the compacted clayey sand used in this study: this value corresponds to a lightly overconsolidated soil (Dunn, Anderson & Kiefer, 1980; Bergado, Sampaco *et al.*, 1991), giving a coefficient of lateral earth pressure at rest K_0 value of 1·3.

Grid pullout tests

The contribution of the frictional resistance over the longitudinal wires to the total pullout resistance of the grid reinforcement was found on average to be only about 10–15%. The pullout resistance of the grid reinforcements was found to

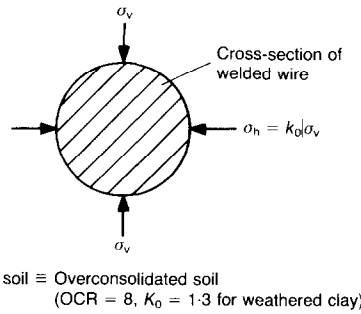

Fig. 16. Average overburden pressure on members of grid reinforcement: $\sigma_{ave} = (\sigma_v + \sigma_h)/2 = 1{\cdot}15\sigma_v$

vary considerably with the *S/D* ratios of the transverse members of the grid. The results of this study agreed essentially with the apparent upper and lower bound envelopes mentioned above, and agreed well with the findings of Ospina (1988). At lower confining normal stresses the failure was closer to the punching shear failure mode; at higher confining normal stresses it was closer to the general bearing failure. For the smaller diameter transverse bars at larger spacings (larger *S/D* values), especially at higher confining normal stresses, the pullout resistances after 25 mm of pull tended to approach the prediction of the general bearing failure mechanism. In the case of the grid mats with closely spaced and larger diameter transverse wires, the pullout resistances after 35 mm pull tended to approach the prediction of the punching shear failure mechanism, especially at low confining normal stresses (Figs 17–19).

On the wet side of OMC, the total pullout resistances were found to be very small. This is reflected by the low values of the shear strength parameters of clayey sand backfill on the wet side (Table 2). Moreover, the clayey sand backfill on the wet side was found to be fully saturated. The increase in the moisture content seems to incline the pullout failure mechanism in front of the transverse bars towards the general bearing failure mechanism (Fig. 19). The pullout behaviour of the grid reinforcements in compacted cohesive–frictional soils on the wet side is comparable with that in loose and dry sands.

Effect of stage loading

The rate of increase in the total pullout resistance with the grid displacement was higher in the earlier part of the laboratory grid pullout tests. After this initial phase, i.e. after about 8–12 mm displacement of the grid specimen, the rate of increase slowed down considerably and the

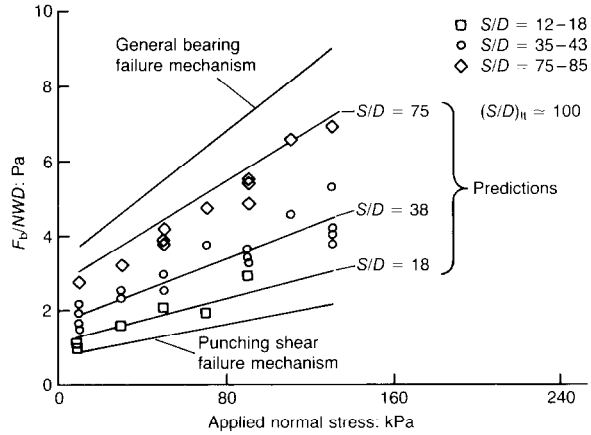

Fig. 17. Grid pullout test results on the dry side of OMC (laboratory, clayey sand)

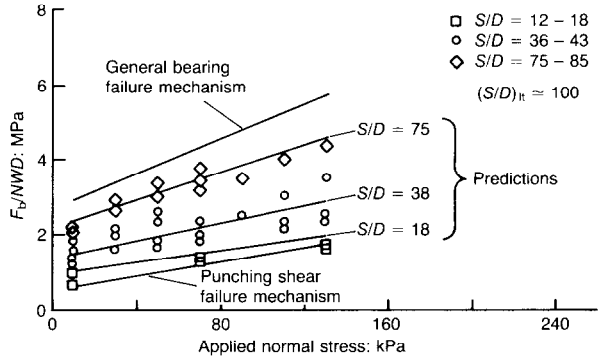

Fig. 18. Grid pullout test results at OMC (laboratory, clayey sand)

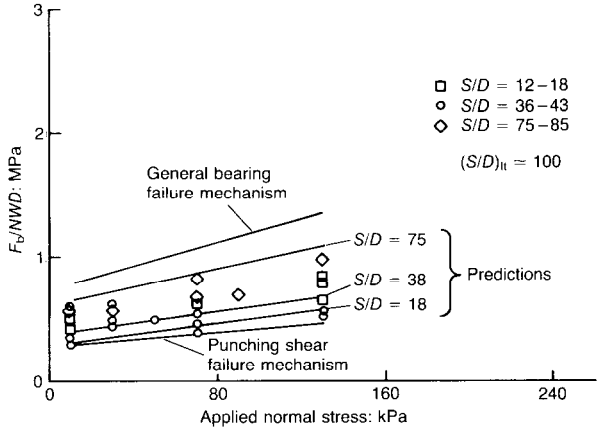

Fig. 19. Grid pullout test results on the wet side of OMC (laboratory, clayey sand)

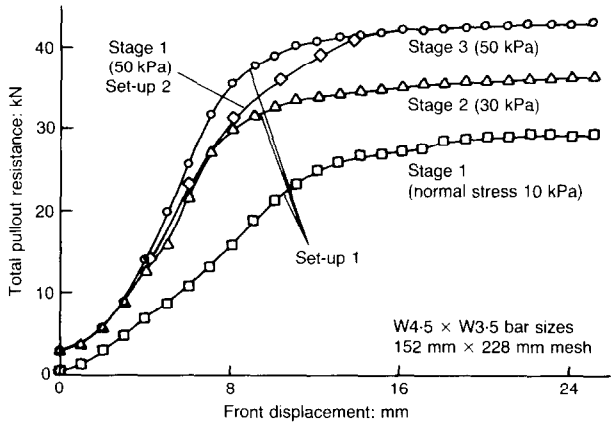

Fig. 20. Typical load–displacement curves from laboratory pullout tests (clayey sand, dry side of OMC)

pullout resistances attained approximately constant values (Fig. 20). For a given displacement at a given normal stress and compaction moisture condition, the laboratory pullout resistance of the grid reinforcements during the first stage loading, especially on the dry side of OMC, was lower than during the later stages (Fig. 20). However, the difference in the maximum pullout resistances at the end of 25 mm of pull was found to be very small. It was therefore concluded from this study that for every stage in a multi-stage pullout testing programme, the maximum pullout resistance at the end of 25 mm of pull for a given normal stress and moisture condition was about the same. The only difference was in the manner in which these peak values were attained. The peak values comprised the maximum pullout resistances of the grid reinforcements at the end of 25 mm of pull, for any set-up at a given moisture condition, adopting the three-stage pullout testing programme for each set-up. The first stage load–displacement curves were found to be flatter and smoother than the later stages, indicating a lower modulus (Fig. 20). The second stage loading results were found to lie on the regression line for the total pullout resistances at that moisture condition (Fig. 21). Motaleb & Anderson (1988) concluded that the load–displacement curves for the multi-stage tests were continuations of the post-yield portion of the first stage curve, which was also found to be relevant to the results of this study.

Degree of interference

Grid members may be considered as a succession of bearing elements buried in the soil that

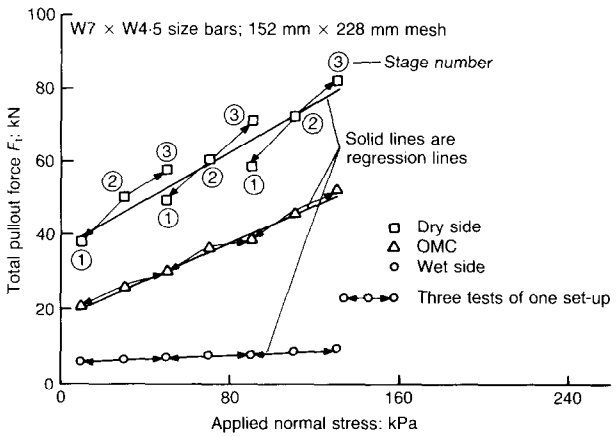

Fig. 21. Effect of moisture content and stage loading on the laboratory pullout capacities (clayey sand)

can interfere with each other (Palmeira & Milligan, 1989). In the calculation of the values of the degree of interference (DI) from the grid pullout test data, the maximum bearing resistance that can be generated in front of the transverse bars with no interference $(F_b/NWD)_{lt}$ was obtained from equations (1)–(3), which give the apparent upper bound value. The DI from the grid pullout test data was thus calculated as

$$\mathrm{DI} = 1 - \frac{(F_b/NWD)_{ave}}{(F_b/NWD)_{lt}} \tag{8}$$

where $(F_b/NWD)_{ave}$ is the average bearing resistance mobilized in front of all the transverse bars of the grid reinforcement obtained from the grid pullout test. The first transverse bar was assumed to have no interference effects; the bearing resistances mobilized in front of all the other transverse bars were assumed to be proportional to the S/D ratios of the grid reinforcement. Therefore, the DI can also be expressed in terms of the grid parameters as

$$\mathrm{DI} = 0{\cdot}8 - \frac{(S/D)}{(S/D)_{lt}} \tag{9}$$

where DI > 0 and $(S/D)_{lt}$ is the limiting value of (S/D) such that for $(S/D) > (S/D)_{lt}$ there will be no more interference effects and the bearing resistances mobilized in front of the transverse members are the maximum possible values. $(S/D)_{lt}$ for clayey sand at all moisture conditions was found to be ~ 100. Equation (9) is valid only for S/D > 10: this was the lower limit value used in the study. The linear relationship of DI and S/D indicated by equation (8) at different compaction moisture conditions is shown in Fig. 22, which also shows that at all moisture conditions, and normal stress levels of 10–130 kPa, the interference between bearing members of the steel grid reinforcements becomes less significant ($< \sim 25\%$) for $S/D > 75$. Although there is considerable scatter in the data, the trend is clear.

PREDICTION EQUATIONS FOR LABORATORY TESTS

The frictional resistance F_f, is given by

$$F_f = \pi LMd[C_a{}^p + \sigma_{ave} \tan(\delta^p)] \tag{10}$$

Dividing both sides by NWD

$$F_f/NWD = \pi S_f[C_a{}^p + \sigma_{ave} \tan(\delta^p)] \tag{11}$$

The terms $C_a{}^p$ and $\tan \delta^p$ were obtained by a simple linear regression of the friction pullout test data with F_f/NWD as the dependent variable and the average overburden pressure, $\sigma_{ave} = 1{\cdot}15\sigma_v$, as the independent variable. The values of $C_a{}^p$ and $\tan \delta^p$ obtained for clayey sand were 70 kPa and 0·18 on the dry side, 37 kPa and 0·05 at OMC and 14 kPa and 0·04 on the wet side.

The bearing resistance in front of the transverse bars has been expressed in general form as

$$F_b/NWD = (CN_c + \sigma_v N_q)(1 - \mathrm{DI}) \tag{12}$$

The term F_b/NWD represents the bearing resistance per unit area of the transverse members normal to the direction of pullout. The bearing capacity factors N_q and N_c were obtained from equations (2) and (3) respectively. The shear strength parameters were derived from the direct shear tests. The DI in equation (12) can be estimated from equation (9) by considering a suitable value of $(S/D)_{lt}$. The prediction lines are shown in Figs 17–19; these agree well with the experimen-

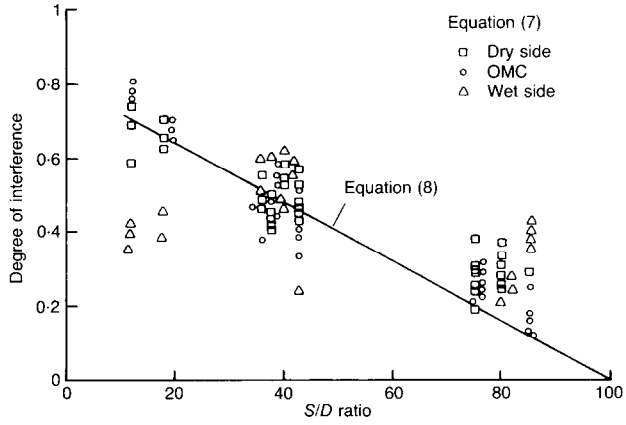

Fig. 22. Variation of degree of interference with S/D (laboratory)

tal data. The total pullout resistance can be expressed in general form as

$$F_t/NWD = [(CN_c + \sigma_v N_q)(1 - DI)] + \pi S_f[C_a{}^p + \sigma_{ave} \tan(\delta^p)] \quad (13)$$

COMPARISON OF LABORATORY AND FIELD RESULTS

The reinforcement mats used in both the laboratory and the field pullout tests had 0·15 × 0·225 m mesh openings with various bar diameters, and most of them had five transverse bars. The length of embedment of the reinforcements in the laboratory pullout tests was ~1·0 m; that of the dummy reinforcements in the field pullout tests was ~2 m. Regular dummy mats 0·15 m × 0·225 m and 2·0 m long were used with some of the transverse bars clipped, and only five or six transverse bars remaining.

Direct comparison of the pullout resistance–pullout displacement curves for field and laboratory pullout tests is difficult because the grid geometry, applied normal pressure, etc. were not exactly the same. Generally, laboratory pullout test curves show a higher resistance mobilization rate and the maximum pullout resistance was mobilized for a pullout displacement of ~20 mm (see Fig. 20). The field pullout tests (see Fig. 12) show a gradual and continuous increase of pullout resistance up to a pullout displacement of more than 50 mm, except for dummy mats 20 and 24. Dummy mat 20 had a higher rate of increase of pullout resistance initially and failed by tension failure of the steel bar. The test results for dummy mat 24 were influenced by slippage of the grips, as indicated in Fig. 12. This difference in pullout resistance mobilization rate is partly because in the field all the transverse members were more than 1 m away from the wall face (the transverse members near the wall face were cut according to the capacity of the pullout machine and to avoid the active zone of the MSE wall), and the formation of the shear surface may need a larger pullout displacement; in the laboratory the pullout box was only 1·25 m long.

For comparison of the field and laboratory maximum pullout resistance per unit bearing area (from transverse members), the resistance for ~1 m ribbed longitudinal members of the field dummy mats in the field was subtracted from total pullout resistance by use of the apparent friction coefficient between ribbed steel bar and clayey sand, which was determined only from field pullout tests with ribbed longitudinal members: the value was 2·77. The field pullout tests yielded higher pullout resistances than the laboratory pullout tests (Table 4, Fig. 23). There are two possible reasons for this

(*a*) the boundary effect as discussed above with reference to the pullout test curves: the first transverse member in the field pullout tests may not be influenced by other transverse members, and may yield a higher bearing resistance (a lower degree of interference)

(*b*) vertical stress redistribution within the reinforced wall/embankment system due to differential settlement of the foundation soil and the bending rigidity of the steel grids. The interconnection of all the reinforcement layers at the facing for the full length and height of the wall, and the fact that the settlements at the middle lateritic soil section were higher than at the two end (clayey sand and weathered clay) sections, might have caused arching effects. These effects might in turn have caused the vertical stresses or the overburden pressures from the middle section to be redistributed to the two end sections. During the laboratory pullout tests, the interaction of the soil/reinforcement system and the rigid boundaries of the laboratory pullout

Table 4. Laboratory and field pullout resistances: mesh 152 mm × 228 m

	Dummy mat number (see Fig. 9(a))				
	24	20	10	9	7
Mat	W7 × W4·5	W4·5 × W3·5	W4·5 × W3·5	W12 × W5	W7 × W4·5
$M \times N$*	4 × 5	4 × 5	4 × 0	4 × 5	4 × 5
Overburden: m	0·50	2·40	3·75	3·80	4·23
Pullout: mm/s	46·0	61·5	127·0	126·0	127·5
Embedment: m	2·086	2·078	2·045	2·046	2·045
P_t‡ (field): kN	23·66‡	73·82¶	24·66	94·0	103·52
P_t‡ (laboratory): kN	31·90	50·4	20·9	69·6	67·2

* M is number of longitudinal bars, N is number of transverse bars.
† P_t is total pullout force.
‡ Not a peak value.
¶ Tension failure at grips.

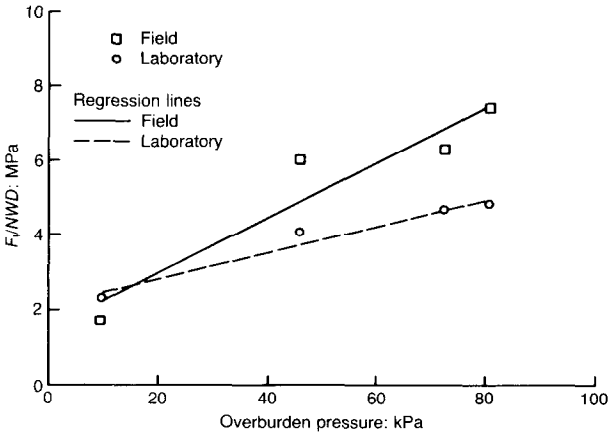

Fig. 23. Comparison of laboratory and field pullout test results (clayey sand)

box, expecially the front face in the small scale tests, can affect the generated pullout resistances. Compaction and moisture can be controlled better in the laboratory.

CONCLUSIONS

The pullout failure mechanisms in front of the transverse members of the grid, and hence the magnitude of the total pullout resistance, were found to be a function of both soil and grid parameters.

Either the general bearing failure mechanism or the punching shear failure mechanism is possible at any time in front of the transverse of the grid during pullout, depending on the grid and soil parameters.

The pullout failure mechanism was found to be a function of the S/D ratios of the transverse bars, the compaction moisture content of the soil and the stiffness of the soil as compared with that of the transverse member. An increase in the moisture content, the vertical normal stresses or the S/D ratios was found to steer incline pullout failure mechanism towards a general bearing failure mechanism.

The bearing resistances in front of the transverse bars of the steel grid constitute about 85–90% of the total pullout resistance; the frictional resistances over the longitudinal wires contribute the rest.

Interference between the passive resistant zones of the successive transverse members in a steel grid reinforcement becomes less significant for S/D ratios greater than ~ 7.5. However, bar diameters of ~ 6.35 mm for both longitudinal and transverse bars forming mesh openings of about 0.15×0.225 m to 0.15×0.3 m have been found to be the most convenient in practice. The vertical spacing can be provided according to the design requirements.

Cohesive–frictional soils compacted to 95% of standard Proctor's density on the dry side of OMC can generate pullout capacities comparable to those of the good quality granular backfill soils.

The welded-wire mats can be used effectively to reinforce low quality cohesive–frictional backfill soils.

ACKNOWLEDGEMENTS

This work was done as a part of a three-year USAID sponsored research project conducted at the Asian Institute of Technology (AIT), Bangkok, Thailand. Thanks are due to Professor Loren R. Anderson and Casan L. Sampaco of Utah State University, Logan, Utah, USA, for their help as research collaborators. Dr Shivashankar was supported by the Japanese Government for the first three years of his study at AIT.

NOTATION

- C cohesion intercept of the backfill soil
- D diameter of the transverse wires of the grid reinforcement
- d diameter of the longitudinal wires of the grid reinforcement
- F_b bearing resistance (force) in front of the transverse wires
- F_f frictional resistance (force) over the longitudinal wires
- F_t total pullout resistance (force) of the grid reinforcement
- f frictional resistance over the longitudinal wires

L length of embedment of the grid reinforcement in the backfill soil
M number of longitudinal wires in the grid reinforcement
N number of transverse wires in the grid reinforcement
N_c, N_q bearing capacity factors
S spacing between grid bearing members
W width of each transverse wire
δ angle of friction between the reinforcement and the soil
ϕ angle of internal friction of the backfill soil
μ^* apparent friction coefficient
σ_{ave} average overburden pressure on members of grid reinforcement
σ_h horizontal normal stress
σ_v vertical normal stress

REFERENCES

Bergado, D. T., Sampaco, C. L., Shivashankar, R., Alfaro, M. C., Anderson, L. R. & Balasubramaniam, A. S. (1991). Performance of a welded wire wall with poor quality backfills on soft clay. *Proc. Geotech. Eng. Congr., Boulder*, pp. 909–922. New York: American Society of Civil Engineers.

Bergado, D. T., Shivashankar, R., Sampaco, C. L., Alfaro, M. C. & Anderson, L. R. (1991). Behavior of welded wire with poor quality, cohesive-frictional backfills on soft Bangkok clay (a case study). *Can. Geotech. J.* **28**, No. 6, 860–880.

Bergado, D. T., Hardiyatimo, H. C., Cisneros, C. B., Chai, J. C., Alfaro, M. C., Balasubramaniam, A. S. & Anderson, L. R. (1992). Pullout resistance of steel geogrids with weathered clay as backfill material. *Geotech. Testing J.* **15**, No. 1, 33–46.

Bergado, D. T., Lo, K. H., Chai, J. C., Shivashankar, R., Alfaro, M. C. & Balasubramaniam, A. S. (1992). Pullout tests using steel grids reinforcement with low-quality backfill. *J. Geotech. Engng. Div. Am. Soc. Civ. Engrs* **118**, No. 7, 1047–1063.

Chang, J. C., Hannon, J. B. & Forsyth, R. A. (1977). *Pullout resistance and interaction of earthwork reinforcement and soil.* Transportation Research Record 640, pp. 1–7. Washington, D.C.: National Research Council.

Dunn, I. S., Anderson, L. R. & Kiefer, F. W. (1980). *Fundamentals of geotechnical analysis.* New York: Wiley.

Jewell, R. A., Milligan, G. W. E., Sarsby, R. W. & Dubois, D. (1984). Interaction between soil and geogrids. *Polymer grid reinforcement*, pp. 18–30. London: Thomas Telford.

Jewell, R. A. (1990). Reinforcement bond capacity. *Géotechnique* **40**, No. 3, 513–518.

Motaleb, A. A. A. & Anderson, L. R. (1988). *Pullout resistance of welded wire mats embedded in clayey silt backfill.* MS thesis, Utah State University.

Ospina, R. I. (1988). *An investigation on the fundamental interaction mechanism of non-extensible reinforcement embedded in sand.* MS thesis, Georgia Institute of Technology.

Palmeira, E. M. & Milligan, G. W. E. (1989). Scale and other factors affecting the results of the pullout tests of grids buried in sand. *Géotechnique* **39**, No. 3, 551–584.

Peterson, L. M. & Anderson, L. R. (1980). *Pullout resistance of welded wire mesh embedded in soil.* Research report, Utah State University.

Schlosser, F. & Elias, V. (1978). Friction in reinforced earth. *Proc. Symp. Earth Reinforcement, Pittsburg*, pp. 735–762. New York: American Society of Civil Engineers.

Shivashankar, R. (1991). *Behavior of a mechanically stabilized earth (MSE) embankment and wall system with poor quality backfills on soft clay deposits, including a study of the pullout resistances.* Doctoral dissertation submitted, Asian Institute of Technology, Bangkok.

Vidal, M. H. (1969). *The principle of reinforced earth.* Highway Research Record 282, pp. 1–16. Washington, D.C.: National Research Council.